ACTIVE CONTOURS AND INFORMATION THEORY FOR SUPERVISED SEGMENTATION ON SCALAR IMAGES

Valérie Duay[1], *Sara Luti*[2], *Gloria Menegaz*[2] *and Jean-Philippe Thiran*[1]

[1]Signal Processing Institute (ITS), Ecole Polytechnique Fédérale de Lausanne (EPFL), CH-1015 Lausanne, Switzerland
http://lts5www.epfl.ch/
[2]Universita' Degli Studi di Siena, 53100 Siena, Italy
http://www.dii.unisi.it/
Email: valerie.duay@epfl.ch, luti.sara@gmail.com, gloria.menegaz@gmail.com, jp.thiran@epfl.ch

ABSTRACT

In this paper, we present two models for supervised scalar image segmentation based on the active contours and information theory. First we propose to carry out a region competition by optimizing an energy designed to be minimal when the entropy of the inside and outside regions of the evolving active contour are close to those of a reference image. The probability density functions (pdfs) used by this model can be computed in a preprocessing step on a reference image. This substantially reduces the computational complexity making this model fast. On the other hand, this implies that the reference image and the image to segment have similar pdfs. When the pdfs are too different or both images are not from the same modality we propose a second segmentation model computationally more expensive but more robust to intensity differences. This second model is based on an information measure extensively used for image registration, the joint entropy. The performance of both models is demonstrated on a variety of 2D synthetic data and medical images. They are also compared in term of segmentation accuracy and computational cost with an entropy-based unsupervised segmentation model recently proposed.

1. INTRODUCTION

Segmentation methods aim to partition an image into a finite number of semantically important regions. This finds a wide range of potential applications in image or video analysis including image or video coding, tracking, object recognition, statistical studies or augmented reality. The segmentation models we propose in this paper have been developed in the active contour framework. This technique consists in finding the curve that minimizes an energy functional designed to be minimal when the curve has reached the object contours.

The first generation of active contour segmentation methods has been based on edge detection [4, 8]. As the evolution of boundary-based segmentation methods depends on local image gradients, they are very sensitive to noise, fuzzy contours or texture edges. To cope with this problem, more robust models using global information about the regions to segment have been proposed. This information is given by a statistical region descriptor. Probably the most well-known region-based model is the 2-phase method based on the mean descriptor presented by Chan and Vese in [11]. Other descriptors have been proposed such the variance [10, 16] or the probability density function (pdf) [12, 15, 17, 19]. For the time being, pdf looks to be the most promising feature to describe a region. Region-based segmentation can be supervised or unsupervised. The segmentation is unsupervised when the region descriptor is only extracted from the image to segment. When the region descriptor is based on a feature of reference, the model is supervised.

This work concerns supervised segmentation models based on pdfs. So far, two main approaches have been presented. The first, presented by Paragios et al in [12], proposes to include in a segmentation model, prior knowledge about the desired intensity properties of the different regions to detect, by minimizing an energy derived from an a posteriori density function. This density function defines the probability that a given pixel belongs to a particular region knowing its intensity value. In [15], Jehan-Besson et al. propose a different approach that consists in minimizing the "distance" between the pdfs of regions selected in the image to segment and pdfs of references. They propose to measure this "distance" with the Kullback-Leibler divergence measure, the Hellinger distance or the chi-2 function comparison function. In this paper, we investigate another important information theoretical measures, the entropy and the joint-entropy, to carry out a two-phase segmentation of scalar images in a supervised way.

The remainder of this paper is organized as follow. In section 2.1, we present the two unsupervised models that Herbulot et al. [17, 19] have proposed for unsupervised segmentation of scalar and vectorial images (color images or motion vector fields). These models are the main source of inspiration for this work. In section 2.2, we show how we adapt these models to perform the segmentation of scalar images based on a reference image. We will see that one of these models used in a supervised way leads to the minimization of energy that has a very close form to the one proposed by Paragios. In section 3, we compare on a variety of 2D synthetic and medical images the performance of the two supervised models we propose with the unsupervised model for scalar image segmentation in [17]. Finally, these three segmentation models are discussed and conclusions are drawn in section 4.

2. METHOD

2.1 The unsupervised segmentation models of Herbulot

In [17, 19], Herbulot et al. propose to carry out the segmentation of gray-scale and vectorial images composed of an object and a background by minimizing the entropy (H) of each region. In this context, the entropy is used to measure the homogeneity of a region.

2.1.1 Segmentation of scalar images

Following the Shannon definition [1] and the non parametric approximation of Ahmad and Lin [3], the marginal entropy[1] on a fixed region Ω is computed as follow:

$$H(q(\Omega)) = \int_{\Omega} \varphi(q(I(x),\Omega))dx, \tag{1}$$

with

$$\varphi(q(I(x),\Omega)) = -\frac{1}{|\Omega|} ln[q(I(x),\Omega))], \tag{2}$$

where $\varphi(.)$ as a region descriptor, $q(I(x),\Omega)$ is the probability density functions (pdf) associated with an observation $I(x)$ for a fixed

[1]The entropy was defined with the neperian logarithm because this logarithm has the simplest derivative: $ln(q)' \rightarrow \frac{1}{q}$.

region Ω at a given moment and $|\Omega|$ is the area of Ω. In this approach, the image intensity $I(x)$ is considered as a random variable.

The pdf of intensity of the region Ω is estimated in a non-parametric way using the Parzen windows method [2]:

$$q(I,\Omega) = \frac{1}{|\Omega|}\int_{\Omega} G_{\sigma}(I - I(\hat{x}))d\hat{x}, \tag{3}$$

where G_{σ} is the Gaussian kernel with 0-mean and σ^2 variance.

Minimizing functional (1) involves the computation of its derivative. By using the shape derivative tool [13, 16], the Eulerian derivative in the direction $\mathbf{V}$ of the criterion (1) corresponds to:

$$< H, \mathbf{V} >= \int_{\Omega} \frac{\partial \varphi(I(x),\Omega,\mathbf{V})}{\partial \tau} dx - \int_{\partial\Omega} \varphi(I(x),\Omega))(\mathbf{V}\cdot\mathscr{N})ds \tag{4}$$

where $\frac{\partial \varphi(I(x),\Omega,\mathbf{V})}{\partial \tau}$ is the shape derivative. The region integral considers the dependence of the criterion with the region Ω and the contour integral considers the dependence of the criterion with the contour $\partial\Omega$.

It is demonstrated in [17, 19] that Equation (4) can be rewrite as the following contour integral:

$$< H, V >= -\int_{\partial\Omega} (A(I(x),\Omega) + B(I(x),\Omega))(\mathbf{V}\cdot\mathscr{N})ds \tag{5}$$

$A(I(x),\Omega)$ is a term coming from the dependance of the descriptor with the region and $B(I(x),\Omega)$ is a term coming from the dependance of the descriptor with the contour.

In our case,

$$A(I(x),\Omega) = -\frac{1}{|\Omega|}\int_{\Omega} \frac{\partial \varphi(q(I(x),\Omega))}{\partial q}[q(I(x),\Omega) - G_{\sigma}(I(x) - I(\hat{x}))]d\hat{x}, \tag{6}$$

with

$$\frac{\partial \varphi(q(I(x),\Omega))}{\partial q} = -\frac{1}{|\Omega|}\frac{1}{q(I(x),\Omega)}, \tag{7}$$

and

$$B(I(x),\Omega) = \varphi(I(x),\Omega). \tag{8}$$

According to the Cauchy-Schwartz inequality, the fastest way to decrease $H(q(\Omega))$ s.t $< H, \mathbf{V} >= \int_{\partial\Omega} F(\mathbf{V}\cdot\mathscr{N})ds$ is obtained by choosing $\frac{\partial C}{\partial \tau} = -F\mathscr{N}$ which leads to the evolution equation:

$$\frac{\partial C}{\partial \tau} = ([A(I(x),\Omega) + \varphi(I(x),\Omega)] + \lambda\kappa)\mathscr{N}. \tag{9}$$

where κ is the curvature of the contour C which regularizes the evolving curve and λ is a weight.

To produce two regions with two pdfs as homogenous as possible, the functional (1) is minimized by using the region competition approach introduced by Zhu and Yuille in [7]. Thus we look for the regions that minimize the following energy:

$$E_H(q_{in}, q_{out}) = H(q(\Omega_{in})) + H(q(\Omega_{out})) + \lambda\int_{\partial\Omega} ds \tag{10}$$

where Ω_{in} is the object region and Ω_{out} is the background region. q_{in} and q_{out} are their corresponding pdfs and $\int_{\partial\Omega} ds$ is the regularization energy.

The energy (10) leads to the following evolution equation:

$$\frac{\partial C}{\partial \tau} = ([A(I(x),\Omega_{in}) + \varphi(I(x),\Omega_{in})] + [A(I(x),\Omega_{out}) + \varphi(I(x),\Omega_{out})] + \lambda\kappa)\mathscr{N}. \tag{11}$$

Solving Equation (11) implies the segmentation of two homogenous regions, which are here the object of interest and the background. In the following of this paper, this marginal entropy-based unsupervised segmentation model will be called ME.

2.1.2 *Segmentation of vectorial images*

For the segmentation of vectorial images, Herbulot proposes another segmentation model based on the joint-entropy. The joint-entropy of a fixed region Ω is computed as follow::

$$H(q(I_1, I_2, \Omega)) = \int_{\Omega} \varphi(q(I_1(x), I_2(x), \Omega))dx \tag{12}$$

with

$$\varphi(q(I_1(x), I_2(x), \Omega)) = -\frac{1}{|\Omega|} ln[q(I_1(x), I_2(x), \Omega))] \tag{13}$$

and

$$q(I_1(x), I_2(x), \Omega) = \frac{1}{|\Omega|}\int_{\Omega} G_{\sigma}(I_1(x) - I_1(\hat{x}), I_2(x) - I_2(\hat{x}))d\hat{x}, \tag{14}$$

where $q(I(x_1), I(x_2), \Omega)$ is the joint probability density functions (pdf) associated with the observations $I(x_1)$ and $I(x_2)$ for a fixed region Ω at a given moment. $G_{\sigma}(.,.)$ is the Gaussian kernel in 2D.

Note that the derivative of the joint-entropy functional (12) is similar to the one of the entropy functional (1). Thus we can directly deduce the evolution equation corresponding to the joint-entropy-based segmentation model by replacing in (11) the probability distribution $q(I(x),\Omega)$ by the joint probability distribution $q(I(x_1), I(x_2), \Omega)$:

$$\frac{\partial C}{\partial \tau} = ([A(I_1(x), I_2(x), \Omega_{in}) + \varphi(I_1(x), I_2(x), \Omega_{in})] + [A(I_1(x), I_2(x), \Omega_{out}) + \varphi(I_1(x), I_2(x)), \Omega_{out}] + \lambda\kappa)\mathscr{N}, \tag{15}$$

where

$$A(I_1(x), I_2(x), \Omega) = -\frac{1}{|\Omega|}\int_{\Omega} \frac{\partial \varphi(q(I_1(x), I_2(x), \Omega))}{\partial q} \cdot [q(I_1(x), I_2(x), \Omega) - G_{\sigma}(I_1(x) - I_1(\hat{x}), I_2(x) - I_2(\hat{x}))]d\hat{x}, \tag{16}$$

with

$$\frac{\partial \varphi(q(I_1(x), I_2(x), \Omega))}{\partial q} = -\frac{1}{q(I_1(x), I_2(x), \Omega)}. \tag{17}$$

In [17, 19], these two entropy-based models were presented to perform unsupervised segmentation, i.e without prior knowledge on the pdfs of the regions to segment. Their pdfs have thus to be recomputed at each iteration of the process to correspond to the regions defined by the current position of the active contour.

2.2 Our supervised segmentation models

In this section, we propose to use the models presented in the previous section to include in a segmentation model prior knowledge about the intensity distribution of the regions to detect. In this work, these prior intensity distributions are extracted from a reference image in which we know the segmentation of the object of interest. This reference image can be either a source image globally put in correspondence to the image to segment with an affine registration (as in the atlas-based segmentation methods [6, 9]) or the previous frame in a video sequence. Note that the reference image gives also to the active contour an initial position close to the target contour. In this supervised segmentation framework, we will call the reference image "atlas" and the image to segment "target image".

2.2.1 Atlas-based marginal entropy model (ABME)

Let q_{prior} be the prior pdf of a fixed region Ω extracted from the atlas.

Inspired by the entropy definition (1), we define the following functional energy $E_{q_{prior}}$ that aims to segment regions having entropies close to the corresponding regions in the reference image:

$$H(q_{prior}) = \int_{\Omega_{in}} \varphi(q_{prior,in}(I(x)))dx + \int_{\Omega_{out}} \varphi(q_{prior,out}(I(x)))dx, \quad (18)$$

with

$$\varphi(q_{prior}(I(x)) = -\frac{1}{|\Omega|} ln[q_{prior}(I(x))], \quad (19)$$

where $I(x)$ is an intensity value of the target image. Thus if the minimization of the energy (18) leads to a perfect segmentation of Ω_{in} and Ω_{out} in the target image, then $q_{in} = q_{prior,in}$ and $q_{out} = q_{prior,out}$.

As q_{prior} is constant, the descriptor $\varphi(.)$ does not depend on the region Ω. Thus, shape derivative $\frac{\partial \varphi(q_{prior}(I(x))}{\partial \tau}$ is equal to zero. The Eulerian derivative in the direction $\mathbf{V}$ of the criterion (18) corresponds simply to the contour integral:

$$< E_{q_{prior}}, \mathbf{V} >= -\int_{\partial\Omega_{in}} \varphi(q_{prior,in}(I(x)))(\mathbf{V}\cdot\mathscr{N})ds - \int_{\partial\Omega_{out}} \varphi(q_{prior,out}(I(x),\Omega))(\mathbf{V}\cdot\mathscr{N})ds. \quad (20)$$

With the region competition and the regularization term we obtain the following evolution equation:

$$\frac{\partial C}{\partial \tau} = -(\varphi(q_{prior,in}(I(x))) - \varphi(q_{prior,out}(I(x))) + \lambda\kappa)\mathscr{N}. \quad (21)$$

This segmentation model assumes that corresponding regions between the reference and target images have similar intensity distributions. When these distributions are too different we propose to use the model described in section 2.2.3.

2.2.2 Related work to ABME

In [12], Paragios et al. presents an energy that has a very close form to the entropy-based energy with prior knowledge (18). The main difference is that they deduce their energy from the a posteriori density function $q(P(\Omega)|I(x))$ describing the membership of a pixel to a particular region following its intensity $I(x)$. $P(\Omega) = \{\Omega_{in}, \Omega_{out}\}$ represents the partition of the image domain into two non-overlapping regions $\{\Omega_{in} \cap \Omega_{out} = \emptyset\}$.

With the Bayes rule, this density function can be rewritten as:

$$q(P(\Omega)|I(x)) = \frac{q(I(x)|P(\Omega))}{q(I(x))} q(P(\Omega)). \quad (22)$$

By assuming that all the partitions are a priori equally possible they ignore the constant terms $p(I(x))$ and $p(P(\Omega))$. Thus the density function (22) becomes:

$$q(P(\Omega)|I(x)) = q(I(x)|P(\Omega)) = q(I_{in}(x)|P(\Omega_{in}))q(I_{out}(x)|P(\Omega_{out})). \quad (23)$$

By assuming that the points within each region are independent they obtain:

$$q(I_{in}(x)|P(\Omega_{in})) = \prod_{\Omega_{in}} q_{prior}(I(x),\Omega_{in}) \quad (24)$$
$$q(I_{out}(x)|P(\Omega_{out})) = \prod_{\Omega_{out}} q_{prior}(I(x),\Omega_{out})$$

Finally, as the maximization of an a posteriori probability is equivalent with the minimization of the $-log()$ function of this probability they get the following functional energy:

$$E(q_{prior}) = -log\left[\prod_{\Omega_{in}} q_{prior,in}(I(x)) \prod_{\Omega_{out}} q_{prior,out}(I(x))\right] \quad (25)$$
$$= -\int_{\Omega_{in}} \varphi(q_{prior,in}(I(x)))dx - \int_{\Omega_{out}} \varphi(q_{prior,out}(I(x),\Omega))dx$$

In conclusion, our a priori entropy-based Energy (18) differs from the a posteriori density function-based Energy (25) by the normalization by the region area.

2.2.3 Atlas-based joint entropy model (ABJE)

In the reference work [19], I_1 and I_2 of the joint entropy-based segmentation model (Equation 15) correspond to two channels of a color image or the components of a 2D dense deformation field. In the model presented here, I_1 corresponds to the target image and I_2 corresponds to the atlas. To be able to compute the joint probability (14), the atlas has to be deformed to follow the evolution of the active contour. During the segmentation process, the atlas I_2 at time t will be thus given by the dense deformation field $u(x,t)$ and the initial reference image $I_2(x,0)$ such that:

$$I_2(x,t) = I_2(x+u(x,t),0) \quad (26)$$

$u(x,t)$ is extracted by tracking the active contour motion. To compute it, we use the level-set based registration method we have previously presented in [18]. In this method, $u(x,t)$ is extracted from the implicit representation of the contour by the level set function ϕ of Osher and Sethian [5]. Let $\phi_T(x)$ be the level set representation of the current active contour and $\phi(x,0)$ be the level set representation of the initial contour. $u(x,t)$ is obtained by solving the following partial derivative equation (PDE):

$$\frac{\partial u(x,t)}{\partial t} = -F\frac{\bigtriangledown\phi}{|\bigtriangledown\phi|}, \quad (27)$$

where

$$F(x,t) = (\phi_T(x) - \phi(x,t)), \quad (28)$$

and

$$\phi(x,t) = \phi(x+u(x,t),0), \quad (29)$$

In fact, $F(x,t)$ measures the distance between the contour represented by $\phi(x,t)$ and the target contours represented by $\phi_T(x)$. Note that when the level set function is carried over by the current deformation field as in (29), the property of signed distance function will be violated as soon as the registration starts and thus causes numerical inaccuracy. In order to avoid this, the level set function $\phi(x,t)$ is re-initialized at each iteration.

Inspired by the optical flow regularization where a Gaussian filtering G_σ is applied on the deformation field at each iteration, the total deformation field is obtained as follows:

$$u(x,t+1) = (u(x,t) + \frac{\partial u(x,t)}{\partial t}) * G_\sigma, \quad (30)$$

where $*$ is the convolution operator. This Gaussian filtering permits to remove discontinuities that appear on the skeleton of the $\phi(x,t)$ due to the distance map property while propagating the correction to the whole deformation field. The Gaussian filtering necessitates to set a parameter σ.

By including the deformation of the reference image in the joint-based segmentation model (15), we obtain the following evolution equation:

$$\frac{\partial C}{\partial \tau} = ([A(I_1(x),I_2(x+u,0),\Omega_{in}) + \varphi(I_1(x),I_2(x+u,0),\Omega_{in})] + [A(I_1(x),I_2(x+u,0),\Omega_{out}) + \varphi(I_1(x),I_2(x+u,0),\Omega_{out})] + \lambda\kappa)\mathscr{N}. \quad (31)$$

3. RESULTS

Figure 1 shows the segmentation results obtained on 2D synthetic images (Rows 1, 2 and 3) and 2D medical images (Rows 4, 5 and 6) with the two supervised models we have presented. Each image has dimensions of 100x100 pixels and pixel dimensions are 1x1 mm^2. These results are compared with those obtained with the unsupervised model for the segmentation of scalar image proposed by Herbulot et al. in [17]. The atlas and the target images are respectively shown in Columns 1 and 2. Column 3 shows the result obtained with the marginal entropy model (ME) (Equation (11)). Column 4 shows the results obtained with the atlas-based marginal entropy model (ABME) (Equation (21)) and Column 5 shows the results obtained with the atlas-based joint-entropy model (ABJE) (Equation (31)). The initial position of the active contour is shown in green on the atlas (Column 1). The segmentation result is shown in green on the images of Columns 3, 4 and 5. The target contours are copied in red onto all of these images to visualize the initial differences and the quality of the segmentation. These target contours, considered as ground truth, were obtained from the target image by manual segmentation. The two values under the images of Columns 3, 4 and 5 represent respectively the number of iterations necessary to obtain the corresponding result and the mask overlap ratio between this automatic segmentation and the ground truth. The value of this ratio ranges from zero to one, with zero indicating no overlap and one indicating a perfect agreement between both masks (for more detail about this mask similarity measure see [14]).

Concerning the results on synthetic images. Row 1 presents synthetic images with two regions gray and black. The corresponding regions between the atlas (Panel 1.1) and the target image (Panel 1.2) have same pdfs. Panels 1.1 shows that the object of interest contains one region, the gray one. In this case, the three models gives similar segmentation results (see Panels 1.3, 1.4 and 1.5). The fastest one is the ABME model because it uses pdfs computed in a preprocessing step on the atlas. Row 2 presents synthetic images containing 3 regions (white, gray and black). Again the corresponding regions between the atlas (Panel 1.6) and the target image (Panel 1.7) have same pdfs. Panel 1.6 shows that the object of interest contain two regions (white and gray). In this case, the ME model segments only the gray region (Panel 1.8). Note that the gray region was the region the most important inside the initial contour (Panel 1.7). The two supervised models segment the same regions that the object of interest in the atlas (see Panels 1.9 and 1.10). Row 3 presents also synthetic images containing three regions but this time the corresponding regions between the atlas (Panels 1.11) and the target image Panel 1.12) have different pdfs. Note that the background of the atlas has the same pdf that the big circle in the target image and conversely. Again, the unsupervised model segments the region the most important inside the initial contour (Panel 1.13). On the other hand, the ABME model segments the background and some points of the object of interest that belongs to its pdfs of reference (Panel 1.14). In this case, only the ABJE model succeeds in the segmentation of the object of interest (Panel 1.15).

Concerning the results on real images. Row 4 presents results on computed tomography (CT) of the neck area. The object to segment in the target image is the jaw. The corresponding regions between the atlas (Panel 1.16) and the target image (Panel 1.17) have similar pdfs. The best results were obtained with the supervised segmentation models (Panels 1.19 and 1.20). The ABME model was the most fast and the most accurate. On the other hand, the ME model segments some homogeneous parts of the tissue surrounding the jaw. Row 5 presents results on brain MR images. The objects to segment in the target image are the lateral ventricles. The reference image (Panel 1.21) and the target image (Panel 1.22) beeing of different modalities (T1 and T2) the corresponding regions have different pdfs. This time, the ME model and the ABJE model succeed in the segmentation of the ventricles. With the ABME model, the active contour tends to disappear as there is no intensity value corresponding to the reference pdf of the ventricles. Row 6 presents results on an anatomical slide. The objects to segment in the target image is the eye. The target image (Panel 1.27) by deforming the atlas with rigid deformation and by changing its window level. Thus it has different pdfs compare to the atlas (Panel 1.26). The best segmentation result was obtained by the ABME model (Panel 1.30). The ME model divides the image in two homogenous regions. Thus the segmented object include part of the tissues surrounding the eyes and presents holes inside the eye. The ABME model segments only the parts of the eye with intensities corresponding to the pdf of reference.

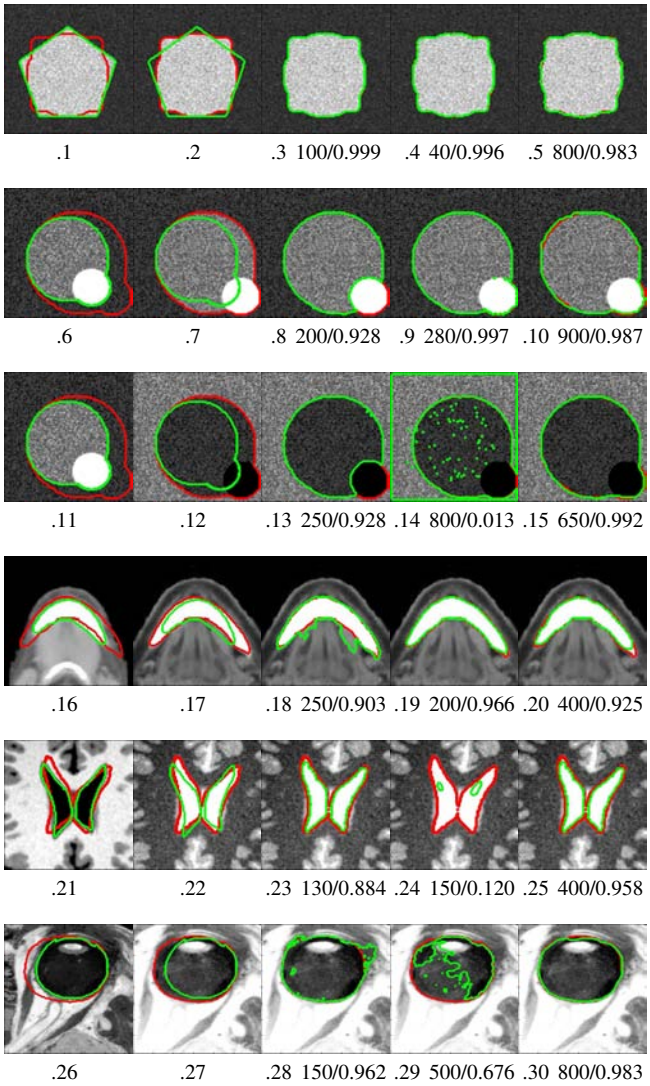

Figure 1: Segmentation results. Columns: 1) Reference image. 2) Image to segment. 3) Unsupervised marginal entropy model (ME). 4) Atlas-based marginal entropy model (ABME). 5) Atlas-based joint-entropy model (ABJE). Rows: 1) Synthetic images: 2 regions, same pdfs. 2) Synthetic images: 3 regions, same pdfs. 3) Synthetic images: 3 regions, different pdfs. 4) Neck CT images: similar pdfs. 5) T1/T2 Brain MR images: different pdfs. 6) Anatomical eye images: different pdfs. Values under the images of Columns 3, 4, 5: Number of iterations/Mask overlap measure.

4. DISCUSSION AND CONCLUSIONS

In this paper, we present two supervised models based on information theory for the segmentation of scalar images. They permit to segment an object in an image by using prior knowledge coming

from a reference image or atlas. These prior knowledge are an initial position for the active contour close to the target contours and prior pdfs concerning the two regions to detect in the target image. The first model based on the entropy addresses the cases where the pdfs of the objects and the background in the reference image are similar to those to segment in the target image. The second model uses the joint-entropy to deal with the cases when these pdfs are too different. Both models are compared with an unsupervised entropy-based model recently proposed by Herbulot et al in [17, 19]. Results showed that when these pdfs are similar the supervised entropy-based model has the lowest computational cost because the pdfs of reference can be computed in a preprocessing step. When these pdfs are too different the supervised joint-entropy based model is the most robust model. On the other hand, this method is more expensive computationally because the joint pdfs have to be computed at each iterations and a second PDE have to be solve to find the deformation field that deforms the reference image to follow the evolution of the active contour. The unsupervised model is faster to deal with different pdfs but the result is very sensitive to the initial position of the contours and the object or the background to segment in the target image have to satisfy the homogeneity criterion. A joint paper [20] illustrates the use of our entropy-based models for an application in volumetric medical images coding. Future work includes using this type of supervised segmentation models to drive the non rigid registration of an atlas as described in [18, 21].

REFERENCES

[1] C. Shannon, "A mathematical theory of communication," in *Bell Sys. Tech. J.*, 27, pp. 379–423, 1948.

[2] E. Parzen, "On Estimation of a Probability Density Function and Mode," in *The Annals of Mathematical Statistics*, 33(3), pp. 1065–1076, 1962.

[3] I. A. Ahmad and P. Lin, "A Nonparametric Estimation of the Entropy for Absolutely Continuous Distributions," in *IEEE Transactions on Information Theory*, 22(3), pp. 372–375, 1976.

[4] M. Kass, A. Witkin, and D. Terzopoulos D, "Snakes: active contour models," in *First international conference on computer vision*, pp. 259–268, 1987.

[5] S. Osher and J. A. Sethian, "Fronts Propagating with Curvature-Dependent Speed: Algorithms based on Hamilton-Jacobi Formulations," in *Journal of Computational Physics*, 79(1), pp. 12–49, 1988.

[6] C.R.J. Maurer et al., "A review of medical image registration," in *Interactive Image-Guided Neurosurgery*, R. Maciunas, Editor. , American Association of Neurological Surgeons: Park Ridge, IL. pp. 17–44, 1993.

[7] S. C. Zhu and A. Yuille, "Region Competition: Unifying Snakes, Region Growing, and Bayes/MDL for Multiband Image Segmentation," in *IEEE Transactions on Pattern Analysis and Machine Intelligence*, 18(9), pp. 884–900, 1996.

[8] V. Caselles, R. Kimmel, and G. Sapiro, "Geodesic Active Contours," in *International Journal of Computer Vision*, 22 (1), pp. 61–79, 1997.

[9] J.B. Maintz and A. Viergever, "A survey of medical image registration," in *Medical Image Analysis*, 2(1), pp. 1–36, 1998.

[10] A. Yezzi, A. Tsai, and A. Willsky, "A Statistical Approach to Snakes for Bimodal and Trimodal Imagery," in *International Conference of Computer Vision*, pp. 898-903, 1999.

[11] T. Chan and L. Vese, "Active contours without edges," in *IEEE Transactions on Image Processing*, 10(2), pp. 266–277, 2001.

[12] N. Paragios and R. Deriche, "Geodesic Active Regions: A New Paradigm to Deal with Frame Partition Problems in Computer Vision," in *Computer Vision. Journal of Visual Communication and Image Representation*, 13(1-2), pp. 249–268, 2002.

[13] G. Aubert, M. Barlaud, O. Faugeras and S. Jehan-Besson, "Image Segmentation using Active Contours: Calculus of Variations or Shape Gradients," in *SIAM Applied Mathematics,*, 63(6), pp. 2128–2154, 2003.

[14] P.-F. DHaese, V. Duay, R. Li , A. du Bois DAische, Th.E. Merchant, A. J. Cmelak, E. F. Donnelly, K. J. Niermann, B. Macq and B. M. Dawant, "Automatic Segmentation of Brain Structures for Radiation Therapy Planning," in *SPIE Medical Image Processing*,pp. 517–526, 2003.

[15] S. Jehan-Besson, M. Barlaud, G. Aubert and O. Faugeras, "Shape Gradients for Histogram Segmentation using Active Contours," in *International Conference on Computer Vision,*, 2003.

[16] S. Jehan-Besson, M. Barlaud and G. Aubert, "DREAM2S: Deformable Regions driven by an Eulerian Accurate Minimization Method for Image and Video Segmentation," in *International Journal of Computer Vision,*,53(1),pp. 45–70, 2003.

[17] A. Herbulot, S. Jehan-Besson, M. Barlaud and G. Aubert, "Shape gradient for image segmentation using information theory," in *ICASSP*, pp. 21–24, 2004.

[18] V. Duay, M. Bach Cuadra, X. Bresson and J. Thiran, "Dense Deformation Field Estimation for Atlas Registration using the Active Contour Framework ," in *EUSIPCO*, 2006.

[19] A. Herbulot, S. Jehan-Besson, S. Duffner, M. Barlaud and G. Aubert, "Segmentation of Vectorial Image Features Using Shape Gradients and Information Measures," in *Journal of Mathematical Imaging and Vision*, 25(3), pp. 365–386, 2006.

[20] G. Menegaz, S. Luti, V. Duay and J.-Ph. Thiran, "An interactive toolbox for atlas-based segmentation and coding of volumetric images," in *SPIE*, 2007

[21] V. Duay, X. Bresson, N. Houhou, M. Bach Cuadra and J.-Ph. Thiran, "Registration of multiple regions derived from the optical flow model and the active contour framework," in *EUSIPCO*, 2007